



# Margin of Safety Based Flood Reliability Evaluation of Wastewater Treatment Plants: Part 2- Quantification of Reliability Attributes

Mohammad Karamouz<sup>1</sup> · Helia Farzaneh<sup>1</sup>

Received: 24 November 2019 / Accepted: 30 March 2020 /

Published online: 12 May 2020

© Springer Nature B.V. 2020

## Abstract

In a companion paper (Part 1), the basic concepts are discussed in details. In this paper, the application of the concepts and the proposed methodology in that paper are utilized to set the strategies in order to quantify reliability attributes. The case study is Hunts Point wastewater treatment plant and its sewershed in Bronx, New York City, so that it could function during flood. The strategies are selected and reliability of the Hunts Point plant is estimated before and after using best management practices (BMPs). Therefore, the copula based non-stationary 100-year flood frequency analysis of rainfall and storm surge analyzed in the companion paper (Part 1), are used to obtain the design values of surge and rainfall. A differential evaluation Markov Chain with Bayesian interface is used in that paper for parameter estimation. Because the co-occurrence of surge and rainfall is more critical in coastal areas, the design value resulted from bivariate analysis has been considered in this study. In this Part 2, a multi-criteria decision making (MCDM) approach, which characterized the uncertainty of sub-criteria in load-resistance concept, is applied. The Margin of Safety (MOS) concept is extended to numerically assess a rather non-probabilistic MCDM evaluation of load and resistance to estimate the reliability of the plant. Finally, Effective strategies are selected for flood hazard mitigation to improve the reliability and performance of the plant. The results present an increase of about 46% in reliability after using BMPs. The framework presented in this paper is applicable to other coastal watersheds and could be a platform for addressing some pressing issues in coastal preparedness with impacts on design criteria of coastal infrastructure.

**Keywords** Coastal flooding · Best management practices (BMPs) · Reliability · Margin of safety (MOS)

---

✉ Mohammad Karamouz  
Karamouz21@gmail.com

Helia Farzaneh  
helia.farzaneh@ut.ac.ir

<sup>1</sup> School of Civil Engineering, University of Tehran, Tehran, Iran

## 1 Introduction

The severity and frequency of nature extremes have recently increased owing to urbanization, population rise, and climate change (Rosenzweig and Solecki 2014). Superstorm Sandy produced the highest water levels recorded in the past 300 years, provoking 43 deaths, \$19 billion asset damage, hospital evacuations, and inundation of public transport stations (Orton et al. 2016; Talke et al. 2014). This paper is the part two of a 2 paper series. In the first paper, a detailed literature review on the concept and the technical aspects of previous work related to statistical and flood frequency analysis was provided Karamouz et al. 2020. In this paper (Part 2), the literature review is concentrated on the previous works related to flood risk management through setting strategies and reliability attributes.

The importance of simulating surface water flows in urban watersheds has led to the development of the physically based hydrologic models. Gridded Surface Subsurface Hydrologic Analysis (GSSHA) is a GIS-based and multidimensional modeling technology developed by the US Army Corps of Engineers for routing rainfall-runoff/flood. It has been used to successfully model extreme flood events in urban and coastal areas (Sharif et al. 2010). These studies found that the model worked best at a grid resolution as small as 30 m and results had high compatibility with FEMA flood inundation maps.

Reliability is a performance indicator that measures the operation of the infrastructure when facing hazards (Alderson et al. 2015; Olyaei et al. 2018). In order to calculate reliability, performance-related criteria, and sub-criteria associated with either design flood load or infrastructure resistance are determined. Many studies have used the load-resistance concept to analyze the impact of extremes, such as blast impact (Stewart et al. 2006), earthquake (Panico et al. 2013), and flooding (Karamouz et al. 2018a). The reliability assessment of infrastructure performance is performed through multi-objective analysis, which provides an appropriate decision-making tool in complex environmental systems (Fu et al. 2013; Kim and Smith 2005). When the water infrastructure components are exposed to uncertainty, the design conditions with certainty are no longer valid. Thus, the conventional deterministic approach is unable to account for the variation likelihood of flood reliability (Niku et al. 1979; Tanyimboh and Templeman 1993). Simonovic and Nirupama (2005) developed a framework by combining the MCDM approach with fuzzy theory to simulate the built-in uncertainty in water resource management. A probabilistic method (e.g., Monte Carlo simulation method) is an alternative to deal with parameter uncertainties in hydrologic modeling. The Monte Carlo simulation allows us to perform a comprehensive probabilistic analysis to assess the uncertainty in hydrologic variables. Karamouz et al. (2018b) carried out an uncertainty analysis on the resilience measurement of coastal WWTPs through probability distribution generation for inputs to the resilience evaluation model. Yet, there is no study on reliability quantification using Monte Carlo simulation to observe the variability in reliability criteria obtained from MCDM based approach for WWTPs. To this end, this study determines the variability of estimated actual value for each criterion using Monte Carlo analysis. For probabilistic reliability assessment, two approaches of Direct Integration and Margin of Safety (MOS) are used. The former approach evaluates the risks for an infrastructure by estimation of statistical parameters of probability distributions of load and resistance through best-fitted distribution functions (Mays 2010), while the latter approach is defined as a random variable through obtaining the difference between the resistance elements and flood design load.

Hazard risk mitigation approaches are developed to protect the communities in the coastal areas (Charlier et al. 2005). These protection measures are classified into three distinct groups: (1) traditional coastal measures (gray infrastructure) including seawalls, revetment, bulkhead, levees,

groins, breakwaters, and jetties (Marfai et al. 2015); (2) soft defense measures such as beach fills, sand bypassing, sand dunes stabilization (Masria et al. 2015); and (3) natural protection works (green infrastructure) such as constructed wetlands, submerged breakwaters, perched beaches, artificial headlands (Tunji et al. 2012). Adaptation of hazard risk management strategies is employed to significantly alleviate the hazard potentials through the integration of conventional flood protection mechanisms as well as flood mitigation, inhibition, and improvement tools (Sharif et al. 2010). Depending on the flood risk requirements associated with the system support, the paired activities of individuals and organizations are combined to deal with the flood risks. These activities include maintaining an interconnection between urbanization, flood protection, and financial support (Sayers et al. 2002). Therefore, Housing and Urban Development committee held a national competition with a principal goal of developing novel solutions to the flood protection management of New York City after Superstorm Sandy, namely, Rebuild by Design (RBD) ("Rebuild by Design organization" 2014). RBD employed an innovative methodology to envision the transformation of the watershed-scale affected area towards the improved resilient region. For further information on the list of proposals, the readers are suggested to refer to (Karamouz et al. 2018b; Šakić Trogrlić et al. 2018; Karamouz and Mohammadi 2020).

While previous studies have assessed the influence of BMP incorporation on hazard mitigation, little attention has been given to the joint effect of extreme events of rainfall and surge. The flood reliability of coastal WWTPs needs to be further investigated to determine how the stochastic nature of certain factors (criteria) could affect the reliability measures. In this study, these shortcomings have been realized. The likelihood of marginal and joint probability of storm surge and rainfall though a DE-MC algorithm (Bayesian inference-based approach) and non-stationary copula approach are investigated. Furthermore, a probabilistic approach to load-resistance concept is proposed to quantify reliability, where the concept of Margin of Safety (MOS) has been applied.

This paper is organized as follows. In the next section, the short summary of the concept and the methodology from part 1 is presented with some more details strategies and reliability attributes. Then, the case study details with data preparation for hydrologic distributed model including modeling set up are described for Hunts Point WWTP sewershed in the Bronx county in New York. Finally, a summary and conclusion is given.

## 2 Methodology

The framework of this study consists of four steps to improve the performance of WWTPs. First, the input data needed for hydrologic modeling is collected. Then, existing trends in the time series of observational data of rainfall and surge are investigated. Besides the univariate analysis, bivariate flood frequency is implemented for the joint effect of rainfall and surge (see Karamouz and Farzaneh (2020) - Part 1). In part 2, the reliability index is defined to assess the performance of the plant. This index could be used to show how the improvement in reliability of coastal protection strategies in terms of best management practices (BMPs). The proposed methodology is used in both papers as shown in Fig. 1. Steps 3 and 4 are discussed and utilized in this paper.

### 2.1 Floodplain Mapping

The first step to delineate floodplain is hydrologic distributed modeling of flood events. Through GSSHA module of the WMS software developed by the USACE, the integration

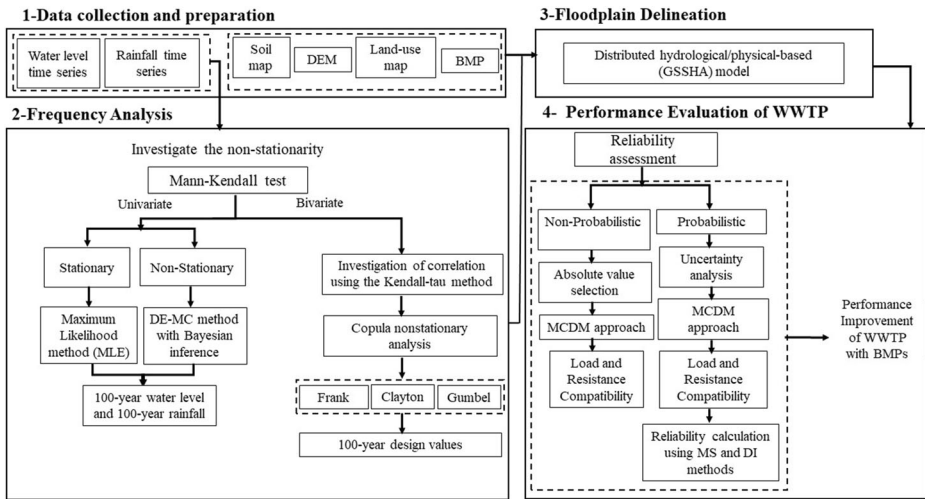


**Fig. 1** Proposed framework for flood reliability of coastal infrastructure/WWTP (Karamouz and Farzaneh (2020) –Part 1)

of GIS-based rainfall-runoff and flood routing model is provided with in-depth details of the characteristics of a watershed (land use and soil type).

## 2.2 WWTP Performance Evaluation

The performance of WWTPs is investigated through reliability calculation by the load-resistance concept. A reliable plant is defined when the applied load is lower than its carrying resistance capacity. Using the MCDM approach, performance-related criteria and sub-criteria are determined to assess a reliability/performance index.

### 2.2.1 Reliability Assessment

The failure of infrastructure occurs when the external load during flood exceeds the resistance of the infrastructure, implying that the system is no longer functional. This study defines the resistance criteria as the potential resistance capacity of the plant, while the load criteria account for the intensity of the design flood. The criteria and sub-criteria associated with load and resistance are defined. The load criteria are categorized into two main classifications: triggers and demands. Triggers (physical load) include the vulnerability criterion such as the longitudinal extent of the infrastructure adjacent to the coastal line), hydrologic criteria such average inundation depth and critical flood elevation, and the quality criterion (treatment biological parameters). The demands category includes additional load during the flood and the population being served.

The resistance criteria are categorized into structural and non-structural sub-criteria. The structural criteria of resistance show the intrinsic capability of a WWTP to perform three stages of treatment on five biological parameters of BOD, COD, TSS, TN, and TP. In the aeration tank, four kinetic coefficients are defined, including the maximum rate of substrate utilization per unit mass of micro-organism ( $k$ ), endogenous decay coefficient ( $k_s$ ), substrate concentration at one-half the maximum growth rate ( $k_d$ ), and yield coefficient over a finite period of log growth ( $Y$ ). The non-structural criteria of resistance are divided into two categories of human

resources (number of staffs) and resiliency (the distance between Hunts Point plant, the nearest WWTP, and the coastal line). The load and resistance criteria are shown in Fig. 7(a) and (b), respectively in the result section for the case study of this paper.

The load and resistance sub-criteria are weighted using the Analytical Hierarchy Process (AHP), a technique developed in Multi-Criteria Decision-Making (MCDM) method. In this study, the weight and values associated with each sub-criterion are applied to an MCDM approach named preference ranking organization method for enrichment evaluation (PROMETHEE) to calculate the reliability of the WWTP (Karamouz et al. 2016). Further information on detailed information of PROMETHEE method can be found in (Balali et al. 2014). In the next step, two auxiliary scenarios are defined to calculate the Hunts Point WWTP performance through the MCDM approach. In the baseline scenario, the inundation depth of a 100-year flood in Hunts Point WWTP is estimated by assuming the critical condition where all biological parameters fail to meet the standard threshold values. The comparisons of the values of load and resistance should be determined to obtain the reliability of the WWTP system. Since the nature of load and resistance are not entirely compatible, the baseline scenario is defined where the load and resistance in Hunts Point are considered to be rescaled. The second scenario is the reliability performance of Coney Island WWTP during a 100-year flood; this scenario is only used for comparison between minimum and maximum values in the MCDM structure.

For reliability estimation using the load-resistance approach, the values of sub-criteria are calculated. The value of water quality indicator is determined using Eq. (1).

$$\text{Water quality indicator} = \sum \left( w_{b_p} \times \frac{b_{pin}}{b_{ps}} \right) \quad (1)$$

where  $w_{b_p}$  is the weight of each biological parameter, and  $b_{pin}$  and  $b_{ps}$  are the initial and standard values of each biological parameter.

Next, the values of effluent biological parameters from each unit are determined using Eq. (2) as suggested by Olyaei et al. 2018.

$$C^{out} = C^{in} \prod_{j=1}^5 (1 - PR_j * PP_j) \quad (2)$$

where  $j$  indicates the number of plant operation units (the total number of units is 5 for Hunts Point WWTP in this study),  $C^{in}$  and  $C^{out}$  are inflow and outflow of each biological parameter (BOD, COD, TSS, TN, and TP), respectively.  $PR_j$  and  $PP_j$  are removal percentage and performance percentage of units (100-failure percentage), respectively.

Failure state of each operation unit depends on its allowable capacity ( $\sigma_a$ ). Performance percentage would be 100 when the inflow to each unit is lower than its allowable capacity. It is assumed that the performance percentage decreases linearly with respect to the maximum influent discharge until the influent discharge reaches  $2\sigma_a$ , where the operational failure occurs and the unit would be no longer functional.

For reliability estimation, two approaches of non-probabilistic and probabilistic are investigated in this study. In the non-probabilistic approach, the load and resistance sub-criteria maintain constant values without uncertainty (Karamouz et al. 2016). However, the effect of parameter uncertainty in estimating load and resistance from a statistical perspective is considered in the probabilistic approach.

**Non-probabilistic Load and Resistance Reliability** In this approach, the values of load and resistance are compared to indicate whether the reliability threshold is passed. BMPs are applied to reduce the load, and improve the reliability of the plant. Load and resistance of the Hunts Point could be comparable using the baseline scenario. To do this, the Hunts Point load value is multiplied by the ratio (R/L) of the baseline scenario, where R and L indicate the resistance and load values, respectively. The reliability status is investigated by comparing the adjusted load ( $L_{\text{adjusted}}$ ) with resistance associated with the Hunts Point WWTP.

**Probabilistic Load and Resistance Reliability** In this study, the stochastic nature of load and resistance factors are evaluated in a non-probabilistic MCDM approach to quantify the reliability. Two approaches are used to account for the uncertainty of the sub-criteria assigned to the MCDM approach. In the first approach, the load sub-criteria with random nature are investigated. In the second approach, random nature is also utilized for resistance. In this study, additional load during the flood and critical flood elevation parameters are incorporated in the load category. For resistance, the potential sources of uncertainty are found in the biological kinetic coefficient of  $k$ ,  $k_d$ ,  $k_s$ , and  $Y$ , which fluctuate within specific ranges (Qasim 1998). The best probability distribution functions are fitted to incorporate the uncertainty of the two load sub-criteria. Uniform distribution is fitted to the four resistance sub-criteria to consider the range of variation of the biological coefficient. These distributions and their corresponding attributes are utilized in a Monte Carlo sampling platform to generate random values.

For each set of random values, the process of load and resistance calculation is repeated and reliability is quantified using Margin of Safety (MOS), and Direct Integration (DI) described in the following sections.

**Margin of Safety (MOS) Method** Margin of safety is used to evaluate the difference between the load and resistance as a random variable (the best-fitted probability distribution function should be determined). From a statistical point of view, reliability is defined as the probability of positive MOS values (i.e.,  $Reliability = P(\text{Resistance} - \text{Load} > 0) = P(MOS > 0)$ ). According to Mays (2010), the reliability index can be calculated as normal deviate of the ratio of the mean and standard deviation of the MOS when the independent load and resistance values along with resulting MOS maintain a normal distribution, as shown in Eq. (3).

$$Z = \frac{\mu_{MOS}}{\sigma_{MOS}} = \frac{\mu_R - \mu_L}{\sqrt{\sigma_L^2 + \sigma_R^2}} \quad (3)$$

where  $Z$  is the standard normal variant,  $\mu_L$ ,  $\mu_R$ , and  $\mu_{MS}$  are the mean values of load, resistance, and margin of safety, respectively;  $\sigma_L$ ,  $\sigma_R$ , and  $\sigma_{MS}$  are standard deviation values of load, resistance, and margin of safety, respectively. When load exceeds resistance, failure occurs in the WWTP. It should be noted that MOS merely employs the nominal average and standard deviations obtained from distributions of load and resistance, which are sufficient to characterize the normally distributed load and resistance. In this study,  $\mu_L$ ,  $\mu_R$ ,  $\sigma_L$ , and  $\sigma_R$  are estimated for the generated load and resistance realizations. In order to calculate the reliability, the standard normal deviate of  $\Phi$  is calculated using Eq. (4).

$$Reliability = p\left(Z \leq \frac{\mu_{MOS}}{\sigma_{MOS}}\right) = \Phi\left(\frac{\mu_{MOS}}{\sigma_{MOS}}\right) \quad (4)$$

where  $Z$  is a standard normal variant and  $p$  is the probability of failure.

**Direct Integration (DI) Method** In this method, according to Mays (2010), the reliability is evaluated using either analytical or numerical integration of the probability density function (pdf) of statistically independent load and resistance in each realization generated by Monte Carlo analysis. Then the reliability can be calculated by Eq. (5).

$$Reliability = \int_0^{\infty} f_R(r) \cdot \int_0^r f_L(l) dl dr = \int_0^{\infty} f_{R_e}(r) F_L(l) dr \quad (5)$$

where  $f_R$  and  $f_L$  are the pdfs of resistance and load, respectively, and the  $F_L$  is the cumulative distribution function (CDF) of the load. In order to estimate the reliability from Eq. (5), the pdf of resistance and CDF of load with the assumption of normal distribution is determined with  $\mu_L$ ,  $\mu_R$ ,  $\sigma_L$ , and  $\sigma_R$  values. This study examines the validity of MOS results by comparing them with the DI method. Mathematica Software developed by Wolfram Research is used to solve the integral.

### 2.3 Flood-Damage Mitigation through BMP Incorporation

One of the practical methods in flood damage reduction is protection measurements, which could reduce the flood-induced damages significantly. According to Hudson River Project's proposal, the flood hazard mitigation practices are classified into four categories of resist, delay, store, and discharge. The store strategy consists of *constructed wetlands* or cisterns to capture excessive runoff at critical facilities such as WWTPs. Due to the low space availability between Hunts Point plant and the coastline, as well as being located in a low-lying area, high elevation levees seems practical.

Implementation of combined levee and constructed wetland structural elements leads to decrease of flood inundation depth in the WWTP area. Among six performance-related load criteria used for reliability quantification, only additional load during the flood and average inundation depth at WWTP are considered.

## 3 Case Study

The Hunts Point plant, shown in Fig. 2 is selected as the focus of this study. This sixty-seven-year-old treatment plant (built in 1952), located on the banks of river alongside Barrette Point Park, treats wastewater from more than half million residents of northeast side of the Bronx. The Bronx is the northernmost point of New York City boroughs, located south of Westchester County and north of Manhattan and Queens. This treatment facility drains approximately 68 km<sup>2</sup> of urbanized land in the eastern section of the Bronx. With a design capacity of 200 million gallons per day (MGD), this facility has one of the lowest altitude among the New York City's WWTPs, which increase the potential of damage due to flood events. The focus of this study is to better understand the impacts of flood hazard mitigation strategies on reducing the risk of flooding through implementation of the two types of BMPs.

Figure 3 demonstrates the New York City sewersheds. In this study, since the Hunts Point plant has a combined sewer system, the sewershed of this plant should be considered that includes Bronx River. The spatial characteristics of the basin are identified with utilization of a DEM of 10 m resolution (USDA 2018). Furthermore, the physical characteristics of different



Fig. 2 Location of Hunts Point WWTP and Bronx River

land uses in the catchment are identified using the soil map of the region, Manning's roughness coefficient for natural channels, soil hydraulic conductivity, and porosity parameters.

## 4 Results and Discussion

### 4.1 Flood Frequency

In this section, based on the correlation between the rainfall and storm surge data, suitable rainfall station is selected to be La Guardia airport station. Then, the existence of non-stationarity is investigated in the time series of surge and rainfall. Using GEV distribution, the extreme value analysis of hydrological data is performed to obtain the design values of storm surge and rainfall (see the companion paper, Karamouz et al. (2020) for more details). In



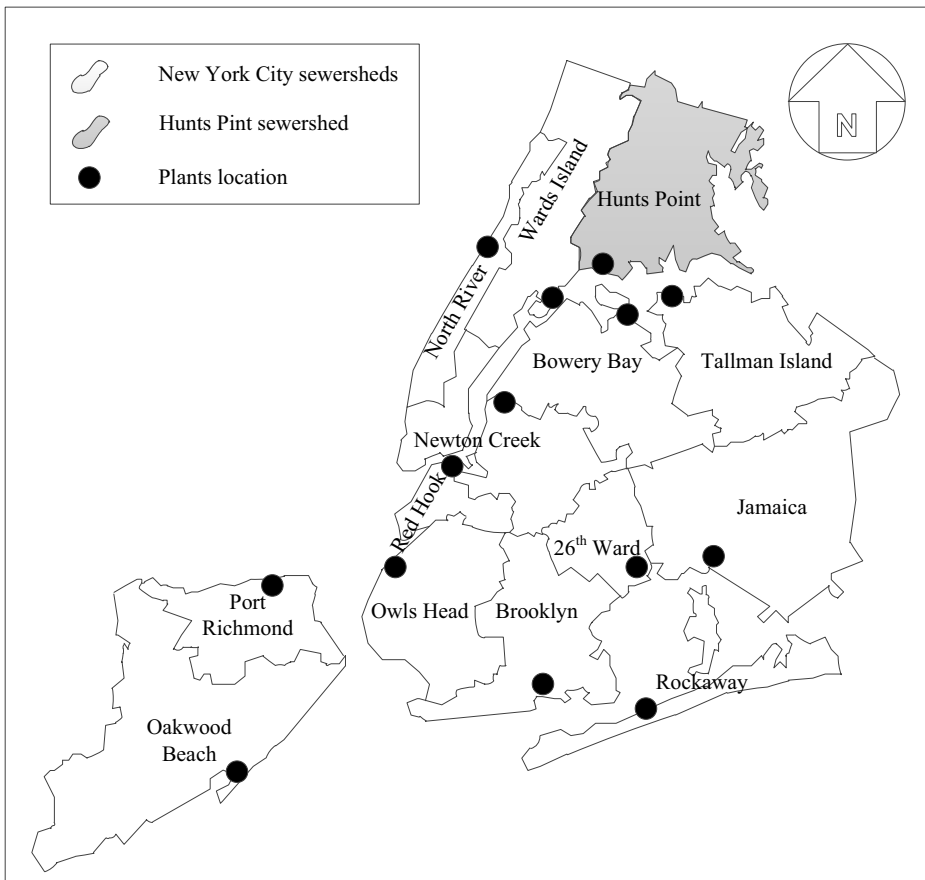


**Fig. 3** Hunts Point sewershed as a part of New York City sewersheds

Fig. 4, the tradeoff for design values of LaGuardia rainfall station are shown. The decision maker has the option to select design values for further analysis.

For the purpose of further analysis, two points that lie on both ends of joint exceedance probability isoline curve ending year 2017 are investigated, as shown in Fig. 4. As shown with dash lines in Fig. 4, these two points have the threshold values: 1) of the highest surge of 2.43 m that corresponds to a rainfall of 50 mm; 2) of the highest rainfall of 160 mm that corresponds to a surge of 1 m. Based on the location of Hunts Point facility, the combined values in “1” has been used for further analysis in this study. It should be noted that the decision-makers could also select the design flood values based on his/her preferences from other curves including the envelope trade-off curve.

After obtaining surge and rainfall design values of 100-year flood, the hydrograph of water level should be introduced to the hydrological model to delineate the floodplain. Karamouz et al. (2018b) has suggested using the hydrograph of Hurricane Irene as the reference flood scenario to obtain the hydrograph of extreme water level for different return periods. Thus, the 100-year surge hydrograph is determined based on the superimposition on the Irene hydrograph, and the effect of astronomical tidal level (measured based on the North American Vertical Datum of 1988). In this study, the flood scenario is based on a surge with the 100-year

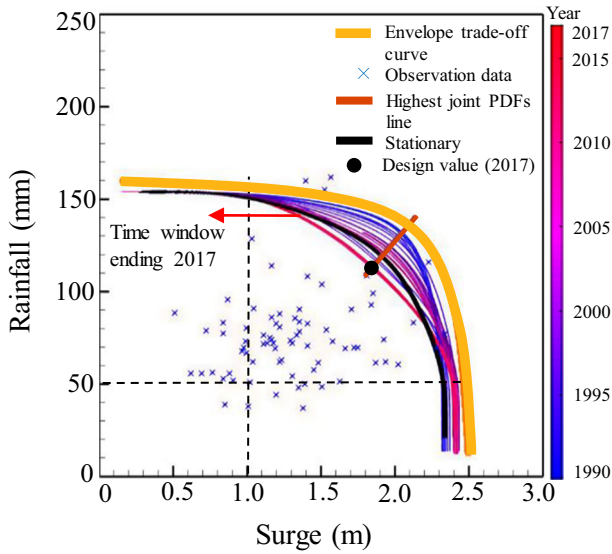


**Fig. 4** Joint exceedance probability-isoline curves for 100-year flood based on MLE parameter estimation for LaGuardia rainfall and Kings Point/Willets Point surge stations in New York City

return period. It is superimposed on the Irene Hydrograph and shown in Fig. 5. To obtain the time series of water level, the effect of astronomical tide is considered. In the second part, a set of coastal protection strategies are employed based on characteristics of the neighborhood.

**4.2 Reliability**

In order to quantify the reliability, the Hunts Point scenario is defined in maximum inundation depth of 2.9 m resulted from GSSHA before using BMPs. Another scenario is considered to make load and resistance of Hunts Point comparable. The inundation depth of this scenario has been calculated 1.9 m. Recalculating reliability index for the Hunts Point plant represents how much it can be improved using BMPs. The effect of BMP is assessed through inundation depth estimation using GSSHA hydrological model. As it is shown in Fig. 6, applying a 3 m-high and 1100 m-long levee and two constructed wetlands of areas of about 3 ha each, the inundation depth at Hunts Point WWTP is decreased. For instance, prior to BMP application, the average inundation depth in the plant location is about 1.8 m. The average inundation depth in the area of Hunts Point WWTP is 0.71 m after the two BMPs application, implying a

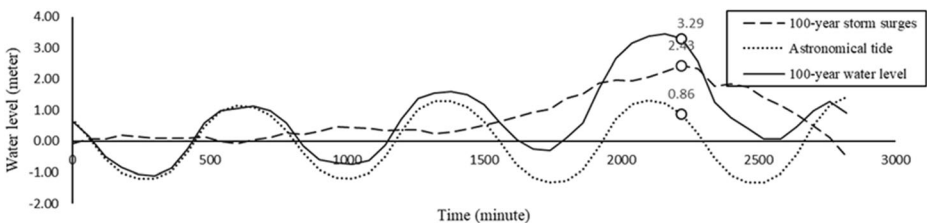


**Fig. 5** Water level hydrograph for 100-year surge based on Irene Hurricane as a reference flood

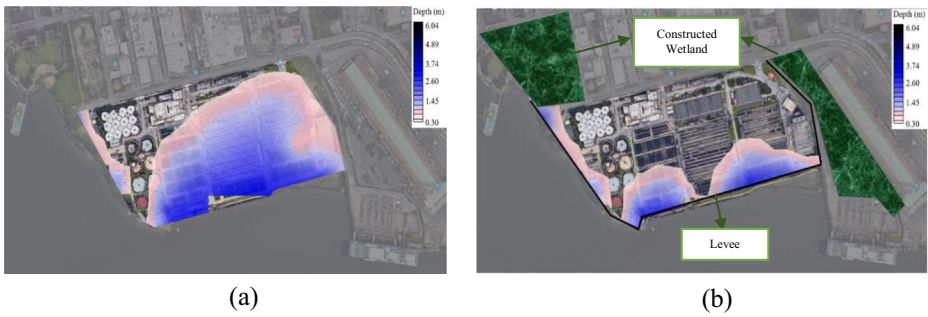


**Fig. 6** Flood inundation depth **a** before, and **b** after application of the two types of BMPs at Hunts Point WWTP

significant reduction of 61%. The inundation depth spatial distribution before and after application of the two types of BMPs have been shown in Fig. 6(a) and (b), respectively.

Using AHP method in the hierarchical framework of load and resistance, the weights associated with load and resistance sub-criteria have been calculated and shown in Fig. 7(a) and (b). The population served and additional load at the time of flooding parameters maintain the two highest weight values due to their effect during the time of flooding. The weight associated with the water quality indicator holds the highest value among other load sub-criteria, as this indicator represents the load quality, which is the primary function of a WWTP to handle.

As shown in Table 1, there are differences in removal percentages for the effluents of the water biological parameters from each OU (such as primary sedimentation tank, aeration tank, and secondary sedimentation tank). The chlorine tank has no effect on the removal of biological parameters (Qasim 1998), so the removal percentage of this unit is zero.

The value of each OU as a resistance sub-criterion is calculated through estimation of performance percentage of each OU using removal percentages of the water biological parameters. To find each OU's value, performance percentage is multiplied by summation of product of removal percentage and associated weight of each biological parameter. In this study, two WWTPs of Hunts Point and Coney Island are studied.

Each plant has a certain capacity to sustain the amount of flow caused by flood, which is called wet capacity. According to Westchester Creek Water body/Watershed Facility Plan Report published in 2011 (New York City Department of Environmental Protection 2011), the values are 17.53 (m<sup>3</sup>/s) and 9.63 (m<sup>3</sup>/s) for Hunts Point and Coney Island WWTPs, respectively. According to Kenward et al. (2013), the total inflow to the Hunts Point and Coney Island plants are selected as 25.612 (m<sup>3</sup>/s) and 21.33 (m<sup>3</sup>/s) based on Superstorm Sandy observations for Hunts Point and Coney Island. For the two plants, the total inflow exceeds their wet capacity, and the excess flow discharges through primary bypass units. The performance percentage (PR) of each OU is calculated as:

$$PR = 100 - \frac{Q_i - Q_{all}}{Q_{all}} \quad (6)$$

where  $Q_i$  and  $Q_{all}$  indicate the flow and allowable capacity of OUs in Hunts Point and Coney Island WWTPs. By subtracting the product of average wastewater flow per capita and population served from the wet capacity, the allowable capacities are estimated as 14.53 (m<sup>3</sup>/s) and 7(m<sup>3</sup>/s) for Hunts Point and Coney Island plants (HES 2014). In Hunts Point plant, after the primary sedimentation tank, there is a secondary bypass unit with a capacity of

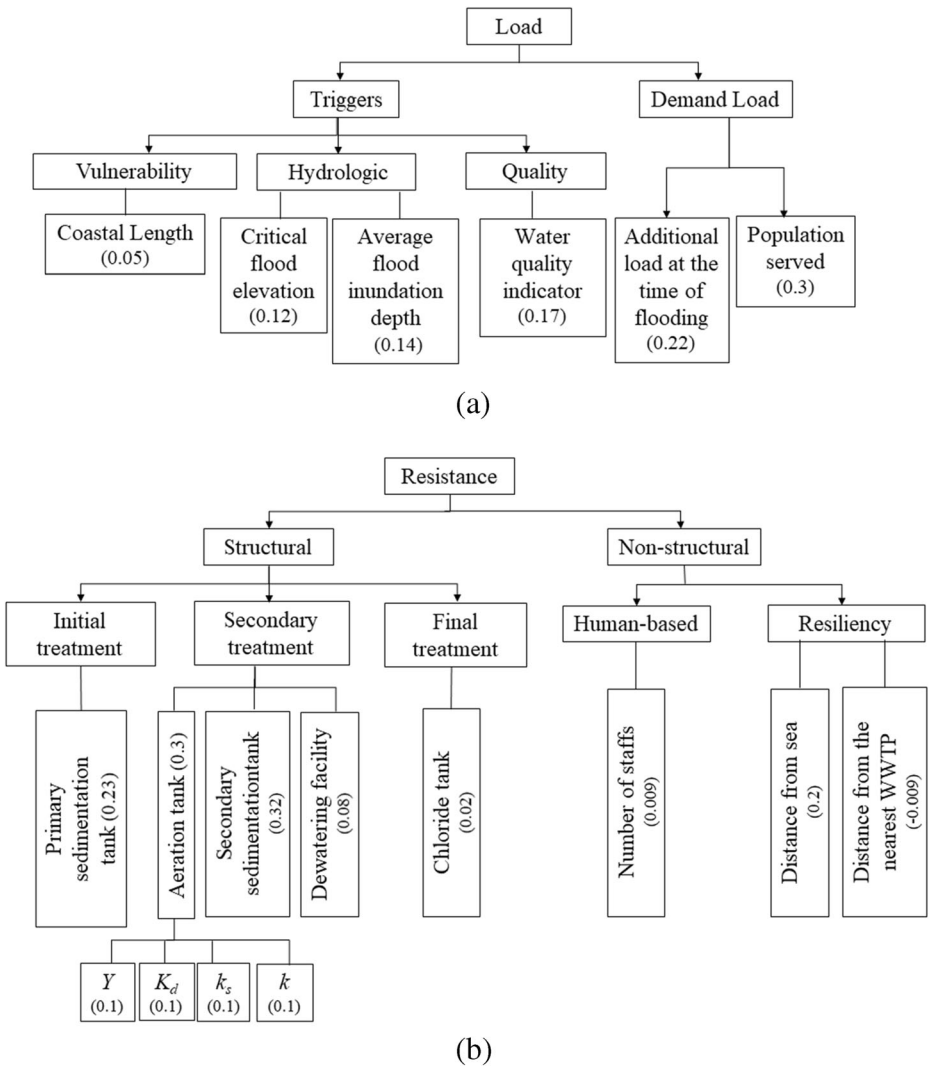


**Fig. 7** Hierarchical categories of **a** load and **b** resistance and the sub-criteria corresponding to each category. Note:  $k$  is the maximum substrate rate;  $K_d$ : delay coefficient;  $k_s$ : substrate concentration;  $Y$ : yield coefficient.

6.13 (m<sup>3</sup>/s) before the aeration tank OU which starts operating when the inflow is more than 11.38 (m<sup>3</sup>/s) according to the Westchester Creek Waterbody/Watershed Facility Plan Report. Also for Coney Island plant, there is a secondary bypass unit, which operates when the inflow is more than 6.25 (m<sup>3</sup>/s). This value is not recorded but assumed based on the product of 11.38 (m<sup>3</sup>/s) and ratio between wet capacities values of Hunts Point and Coney Island plants. The PR value for each OU in the two plants of Hunts Point and Coney Island are shown in Table 2.

The values for factors associated with load and resistance are listed in Table 3 and Table 4. For Hunts Point Scenario, the values of average inundation depth and additional load during flood are dependent on the outputs of GSSHA software. Subsequently, these values for

**Table 1** Weights of water biological parameters and the removal percentages in the operating unit (OU): a) Primary sedimentation tank, b) Aeration tank, c) Secondary sedimentation tank

Biological parameters	Weight of indicator	Removal % of OU (Hunts Point)	Removal % of OU (Coney Island)
a			
BOD	0.24	35	35
COD	0.28	65	35
TSS	0.28	65	0
TN	0.12	25	60
TP	0.08	35	0
b			
BOD	0.24	50	50
COD	0.28	35	50
TSS	0.28	20	20
TN	0.12	30	30
TP	0.08	10	10
c			
BOD	0.24	55	60
COD	0.28	85	60
TSS	0.28	85	75
TN	0.12	10	6
TP	0.08	7	15

baseline and Coney Island scenarios are calculated by normalizing with respect to the ratio of pre-defined inundation depth in Hunts Point Scenario. The existence of dewatering facility unit for each plant (0 represents no availability, whereas 1 indicates the availability) is utilized in the treatment process (Table 4).

**Non-probabilistic Load and Resistance Reliability** The reliability status is listed as *passed* when the difference of resistance and load (R-L) is positive. The resistance sub-criteria are assumed to be constant as 4 (1/d), 0.05 (1/d), 80 (mg/l), and 0.5 (g/g) for  $K$ ,  $k_d$ ,  $k_s$ , and  $Y$  coefficients, respectively according to Metcalf and Eddy (2003). After BMP application, the values of two load sub-criteria, namely average inundation depth obtained by GSSHA and additional load during flood have been changed to 0.71 m and 3.28 ( $m^3/s$ ), respectively.

The resistance value is 48.22, but load value has been reduced from 71.54 to 37.52 after using BMPs. Finally, the load value of Hunts Point as described in the methodology section has been multiplied by the ratio of (R/L) for the baseline scenario to compare the adjusted load ( $L_{\text{adjusted}}$ ) with resistance. The value of  $L_{\text{adjusted}}$  has been calculated 88 and 39.67 before and after BMPs application, respectively. Therefore, the Hunts Point plant would not meet the reliability criteria without BMP application, whereas with BMP implementation, it passes the simple load threshold.

**Table 2** The performance percentage of OUs in Hunts Point and Coney Island plants

	Primary sedimentation tank	Aeration tank	Secondary sedimentation pond
Performance percentage of OUs in Hunts Point (%)	58.80	100	100
Performance percentage of OUs in Coney Island (%)	63.05	100	100

**Table 3** Sub-criteria values associated with load in Hunts Point and Coney Island WWTPs

Sub-criteria	Hunts Point WWTP	Baseline Scenario	Coney Island WWTP
Population served	684,569	684,569	596,326
Water quality indicator	4.54	4.54	6.51
Additional load during flood ( $\frac{m^3}{s}$ )	8.76	5.37	4.82
Average inundation depth (m)	1.8	1.10	1.72
Critical flood elevation (m)	5.34	5.34	4.73
Coastal length (m)	914.13	914.13	467

**Probabilistic Load and Resistance Reliability** The non-probabilistic MCDM method is applied to load and resistance variables to extend the concept of Margin of Safety (MOS). Fourteen WWTPs located in the coastal area of New York City has exhibited ranges of variation for the additional load at the time of flooding and critical flood elevation. In order to simulate the uncertainty in load, first, the best-fitted distribution functions to two above mentioned load sub-criteria are investigated. Weibull and GEV distributions are selected based on the chi-square goodness-of-fit test as the best-fitted functions, respectively.

After the two BMPs application, additional load at the time of flooding is the only load sub-criterion with uncertainty that is affected by reduction of inundation depth. The distribution function of this sub-criterion is estimated by multiplying the values of sub-criteria with random nature obtained from 14 WWTPs by the ratio of average inundation depth after and before the two BMPs application (i.e.,  $0.71/1.8 = 0.4$ ) in order to offset the effects of those sub-criteria when the two BMPs is used. However, for second sub-criterion with random nature is remain unchanged.

The Monte Carlo sampling method is employed to carry out the reliability analysis for Hunts Point WWTP under the two approaches. In the first approach, uncertainties are only considered for load sub-criteria. Using Monte Carlo simulation, 100 realizations of load for Hunts Point and baseline Scenarios associated with one another have been generated. The resistance of Hunts Point have been rescaled using load realizations for baseline scenarios and its resistance value to make load value comparable with resistance. The rescaling procedure consists of multiplying the resistance of Hunts Point Scenario with the ratio of each load over

**Table 4** Sub-criteria values associated with resistance in Hunts Point and Coney Island WWTPs

Operation Units	Hunts point WWTP	Baseline Scenario	Coney Island WWTP
Primary sedimentation tank	29.75	50.6	16.01
Aeration tank	31.80	31.80	22.70
Secondary sedimentation tank	69.76	69.76	34.12
Chlorine tank	0	0	0
Dewatering facility	1	1	0
$K(1/d)$	2–8	2–8	2–8
$k_d(1/d)$	0.03–0.07	0.03–0.07	0.03–0.07
$k_s(mg/l)$	40–120	40–120	40–120
$Y(g/g)$	0.3–0.7	0.3–0.7	0.3–0.7
Distance from the shoreline (m)	23	23	86.53
Number of staffs	108	108	69
Distance to the nearest WWTP(km)	7.97	7.97	2.43

resistance in the baseline scenario. The outcome of this analysis is an estimation of reliability of Hunts Point Scenario without and with BMP implementation.

After fitting a normal distribution to pdf curves of load and resistance, the distribution parameters in MOS method have been estimated. This approach results in the reliability value of 8.38%.

The DI method, however, is obtained by integration of the production function of CDF of load and pdf of resistance, shown in Fig. 8(a) and (b). With a good agreement with the result of MOS method, the reliability value obtained from DI method is estimated as 8.33%. After BMPs application, the reliability values of Hunt Point WWTP obtained from the MOS and DI methods are equal to 43.64% and 43.45%, respectively, which indicates a promising agreement between these two approaches. After using two BMPs, the reliability value calculated from DI method is confirming its compatibility with the MOS method to estimate reliability. The results indicate that after application of the two BMPs, the reliability of WWTP has been enhanced by 36%.

As a second approach to uncertainty analysis in reliability estimation, both resistance and load are considered to be uncertain. Range of uncertainties for four biological kinetic coefficients of  $K$ ,  $k_d$ ,  $k_s$ , and  $Y$  are obtained from Qasim (1998) and have been shown in Table 4. In this approach, 100 realizations for both of the load and resistance of the Hunts Point and baseline scenarios have been generated by Monte Carlo simulation. These values in Hunts Point and baseline scenarios are corresponded with each other based on the order of generation. In order to make the resistance comparable with load in Hunts Point, each load value is rescaled through the multiplication of this value with the ratio of resistance over load for the baseline scenario. As a result, this analysis leads to generation of 100 data sets in which 100 realizations for both load and resistance have been made. The normal distribution is fitted to the load and resistance in each data set to calculate the reliability through margin of safety (MOS). In 80 and 40 out of 100 data sets, the resistance is greater than load with and without application of two BMPs and with the average reliability of 0.84 and 0.45 using MOS method. This shows an almost 46% improvement which is remarkable.

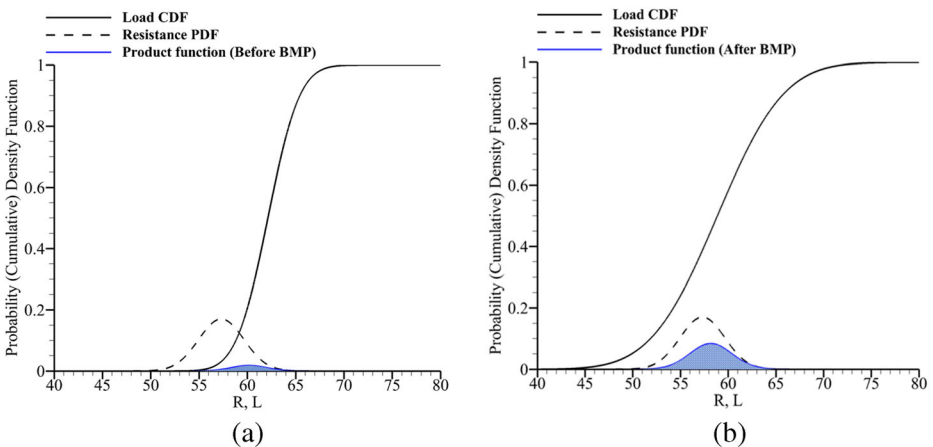


**Fig. 8** The uncertainty-based estimation of reliability using DI approach in Hunts Point WWTP without (a) and (b) with the application of the two BMPs

## 5 Summary and Conclusion

The frequent occurrence of extreme hydrologic events in coastal areas justifies the necessity of evaluating the performance of critical infrastructures, including the wastewater treatment plants in order to find an appropriate mitigation strategy for improving their performance. In this study, to deal with the substantial damages, the best management practices (BMPs) as hazard mitigation strategies are applied. Based on the proposed framework, the reliability index under the deterministic and probabilistic assumptions is quantified to assess the performance of Hunts Point plant in Bronx, one of the five boroughs of New York City. The identified criteria, which are effective on the plant reliability, categorized into load and resistance and can be used to quantify this index. Through using the load-resistance concept based on MCDM and statistical methods of Margin of Safety (MOS) and Direct Integration (DI), the uncertainty-based reliability of the plant is estimated. A GIS-based integrated hydrologic model named GSSHA is applied to determine inundation depth at Hunts Point plant. Results of data analysis in part 1 show the surge data to be non-stationary and rainfall data to be stationary. To obtain the extreme values of rainfall and surge in the 100-year flood, the GEV distribution is applied. In Part 1 GEV parameters are estimated, Using Maximum likelihood method (MLE) for stationary analysis and Differential Evaluation Markov chain Bayesian-based for non-stationary analysis. A series of trade-off curve of rainfall and surge are developed for each time window. In copula non-stationary 100-year flood analysis, the design value for the year of 2017 is determined according to the trade-off curves. For the design of BMPs in coastal areas, extreme surge values and the corresponding rainfall are selected for the last year of record (2017).

The selected BMPs are a combination of a levee and two constructed wetlands for considering the combined mitigation strategies of resist, drainage, and storage effects. The results show how the reliability could be quantified and improved utilizing the concept of MOS and load and resistance attributes. They also show how the proposed methodologies and strategies could positively affect the coastal flood preparedness planning.

**Acknowledgments** Authors would like to thank Dr. M. A. Olyaei, A. Ansari, and K. Mohammadi from the University of Tehran for their valuable comments in preparation of this paper. All input data used in this research can be found from the publicly-available domains of National Oceanic and Atmospheric Administration (NOAA) data center (<http://www.ncdc.noaa.gov/data-access>), NOAA climate prediction center (<http://www.cpc.ncep.noaa.gov/data/indices>), NOAA tides and current <https://tidesandcurrents.noaa.gov/> and U.S. Geological Survey (USGS) national map service (<http://viewer.nationalmap.gov/basic>).

## Compliance with Ethical Standards

**Conflict of Interest** None.

## References

- “Rebuild by Design Organization.” (2014). <<http://www.rebuildbydesign.org/our%0A-work/sandyprojects>> (Nov. 7, 2017)
- Alderson MP, dos Santos AB, Mota Filho CR (2015) Reliability analysis of low-cost, full-scale domestic wastewater treatment plants for reuse in aquaculture and agriculture. *Ecol Eng* 82:6–14
- Balali V, Zahraie B, Roozbahani A (2014) A comparison of AHP and PROMETHEE family decision making methods for selection of building structural system. *Am J Civil Eng Archit* 2(5):149–159
- Charlier RH, Chaineux MCP, Morcos S (2005) Panorama of the history of coastal protection. *J Coast Res*:79–111
- Fu G, Kapelan Z, Kasprzyk JR, Reed P (2013) Optimal Design of Water Distribution Systems Using Many-Objective Visual Analytics. *J Water Resour Plan Manag* 139(6):624–633



- HES (Health Education Service) (2014). "Recommended standards for wastewater facilities" A Report of Committee of the Great Lakes - Upper Mississippi River, Board of State and Provincial Health and Environmental Managers, Albany, USA. [https://www.health.state.mn.us/communities/environment/water/docs/tenstates/wstewtrstnds2014\\_secured.pdf](https://www.health.state.mn.us/communities/environment/water/docs/tenstates/wstewtrstnds2014_secured.pdf)
- Karamouz M, Rasoulnia E, Zahmatkesh Z, Olyaei MA, Baghvand A (2016) Uncertainty-based flood resiliency evaluation of wastewater treatment plants. *J Hydroinf* 18(6):990–1006
- Karamouz M, Rasoulnia E, Olyaei MA, Zahmatkesh Z (2018a) Prioritizing Investments in Improving Flood Resilience and Reliability of wastewater treatment infrastructure. *J Infrastruct Syst* 24(4):04018021
- Karamouz M, Taheri M, Mohammadi K, Heydari Z, Farzaneh H (2018b) "A New Perspective on BMPs' Application for Coastal Flood Preparedness." World Environmental and Water Resources Congress 2018. American Society of Civil Engineers, Reston, pp 171–180
- Karamouz M, Mohammadi K (2020) Nonstationary based framework for performance enhancement of coastal flood mitigation strategies. *Journal of Hydrologic Engineering* 25(6):04020020. [https://doi.org/10.1061/\(ASCE\)HE.1943-5584.0001918.c](https://doi.org/10.1061/(ASCE)HE.1943-5584.0001918.c)
- Karamouz M, Farzaneh H, Dolatshahi M (2020) Margin of safety based flood reliability evaluation of wastewater treatment plants: Part 1 – Basic Concepts and Statistical Settings. *Water Resour Manage* 34:579–594. <https://doi.org/10.1007/s11269-019-02465-8>
- Kenward A, Yawitz D, Raja U (2013) Sewage overflows from hurricane Sandy. Climate Central, Princeton
- Kim K-J, Smith RL (2005) Systematic procedure for designing processes with multiple environmental objectives. *Environ Sci Technol* 39(7):2394–2405
- Marfai MA, Sekaranom AB, Ward P (2015) Community responses and adaptation strategies toward flood hazard in Jakarta, Indonesia. *Nat Hazards* 75(2):1127–1144
- Masria A, Iskander M, Negrin A (2015) Coastal protection measures, case study (Mediterranean zone, Egypt). *J Coast Conserv* 19(3):281–294
- Mays, L. W. (2010). "Water resources engineering." John Wiley & Sons
- Metcalfe, Eddy (2003) *Wastewater Engineering, Treatment and Reuse*, 4th edn. New York: McGraw Hill
- New York City Department of Environmental Protection, (2011) "Westchester Creek Waterbody/Watershed Facility Plan Report", Bureau of Wastewater Treatment, New York, NY. <http://www.hydroqual.com/projects/ltcp/wbws/westchester.htm>
- Niku, S., Schroeder, E. D., and Samaniego, F. J. (1979). "Performance of activated sludge processes and reliability-based design." *Journal (Water Pollution Control Federation)*, JSTOR, 2841–2857
- Olyaei MA, Karamouz M, Farmani R (2018) Framework for assessing flood reliability and resilience of wastewater treatment plants. *J Environ Eng* 144(9):04018081
- Orton, P. M., Hall, T. M., Talke, S. A., Blumberg, A. F., Georgas, N., and Vinogradov, S. (2016). "A validated tropical-extratropical flood hazard assessment for New York Harbor." *Journal of Geophysical Research: Oceans*
- Panico A, Lanzanoa G, Salzano E (2013) Seismic vulnerability of wastewater treatment plants. *Chem Eng* 32
- Qasim S (1998) *Wastewater treatment plants: planning, design, and operation*. CRC Press, Boca Raton
- Rosenzweig C, Solecki W (2014) Hurricane Sandy and adaptation pathways in New York: lessons from a first-responder city. *Glob Environ Chang* 28:395–408
- Šakić Trogrlić R, Rijke J, Dolman N, Zevenbergen C (2018) Rebuild by Design in Hoboken: a design competition as a means for achieving flood resilience of urban areas through the implementation of green infrastructure. *Water* 10(5):553
- Sayers, P. B., Hall, J. W., and Meadowcroft, I. C. (2002). "Towards risk-based flood hazard management in the UK." *Proceedings of the institution of civil engineers-civil engineering*, Thomas Telford Ltd, 36–42
- Sharif HO, Sparks L, Hassan AA, Zeitler J, Xie H (2010) Application of a distributed hydrologic model to the November 17, 2004, flood of Bull Creek watershed, Austin, Texas. *J Hydrol Eng* 15(8):651–657
- Simonovic SP, Nirupama (2005) A spatial multi-objective decision-making under uncertainty for water resources management. *J Hydroinf* 7(2):117–133
- Stewart MG, Netherton MD, Rosowsky DV (2006) Terrorism risks and blast damage to built infrastructure. *Nat Hazards Rev* 7(3):114–122
- Talke SA, Orton P, Jay DA (2014) Increasing storm tides in New York Harbor, 1844–2013. *Geophys Res Lett* 41(9):3149–3155
- Tanyimboh TT, Templeman AB (1993) Optimum design of flexible water distribution networks. *Civ Eng Syst* 10(3):243–258
- Tunji LAQ, Hashim AM, Wan Yusof K (2012) Shoreline response to three submerged offshore breakwaters along Kerteh Bay coast of Terengganu. *Res J Appl Sci Eng Technol* 4(16):2604–2615
- USDA. (2018). "Geospatial data gateway: order data for NY"